Characterization and Corrosion Performance of Powder Coated Aluminium Alloy†

S. Mojtaba Mirabedini[1,2,*], Siamak Moradian[3], J. David Scantlebury[2], and George E. Thompson[2]

(1) Department of Colour, Resins and Surface Coatings, Iran Polymer and Petrochemical Institute, P.O. Box: 14185/458, Tehran, I.R. Iran

(2) Corrosion and Protection Centre, University of Manchester Institute of Science and Technology (UMIST), Manchester M60 1QD, UK

(3) Department of Polymer Eng., Amir Kabir University of Technology, P.O. Box: 15875-4413 Tehran, I.R. Iran

Received 15 May 2001; accepted 11 March 2003

ABSTRACT

The thermal behaviour of an epoxy/polyester powder coating was studied by using differential scanning calorimetry (DSC). Fourier transform infra-red spectroscopy (FTIR) method was employed to evaluate the processes occurring prior to and after curing process. Electrochemical impedance spectroscopy (EIS) was employed to assess performance of differently pretreated powder coated aluminium alloy substrates. The DSC method allows the description of powder coating systems. The spectra showed that the curing process starts at approximately 150ºC and terminates at about 250ºC. According to the impedance data, relatively good performance of the powder coating is due to a high ohmic resistance of the coating prior to and after saturation with water. The data also revealed a better performance of the degreased samples compared to samples treated with polyacrylic acid (PAA). Samples treated with PAA + H_2ZrF_6 (PZr) have shown corrosion inhibition over 60 days of immersion time. Corrosion protection was observed for chromate/phosphate conversion coated (CPCC) samples even after completion of the test.

Iranian Polymer Journal, **12** (4), 2003, 261-269

Key Words:
aluminium;
pretreatment;
powder coatings;
corrosion;
polyacrylic acid.

INTRODUCTION

Due to environmental concerns with organic solvents released to the atmosphere, powder coatings, are replacing more and more solvent-based coatings [1-2]. Powder coatings offer several advantages including little or no volatile organic content, high utilization rates, energy savings, and elimination of hazardous wastes [3]. Powder coatings are usually applied with an electrostatic spray gun to produce thin coatings for decorative and protective purposes. Organic coatings are wide-

(†) Some parts of this work have been presented in 5th Int. Symp. on Electrochemical Impedamce Spectroscopy (EIS 2001) Marilleva, Italy, 17-22, (June 2001).

(*) To whom correspondence should be addressed. E-mail: M.Mirabedini@ippi.ac.ir

ly used to protect metals against corrosion. This is mainly due to their simple application; a low cost of production and provisions of attractive finishes. The efficiency of protection is affected by a number of properties of the total coated system, which consists of paint layer(s), the nature of substrate and its pretreatments [4]. Corrosion of the substrate beneath a paint film can and does still occur. The type of corrosion that may be encountered is usually a function of the coating and the substrate type; the treatment (or lack thereof) of the substrate interface prior to coating application and the environment to which the finished product is exposed to.

Mayne [5] has shown that polymeric coating films are permeable to both water and oxygen. He calculated that the diffusion of water through the polystyrene film was of the order of 10 times greater than that necessary to support the unpainted corrosion rate of mild steel in seawater (0.070 g Fe/cm^2/yr). It was shown that the diffusion rate of oxygen was of the same order as that required by the un-coated steel in sea-water. The film resistance is sensitive to the presence of ions, absorbed from the surroundings, because the ions serve as charge carriers in the film. Thus, the film resistance may give an indication of whether the film could be anticipated to be protective or not. As aqueous corrosion reactions are always electrochemical in nature, the use of electrochemical methods plays an important role in the evaluation of the corrosion performance of coated metal substrates.

Ac Impedance measurements can provide a wealth of kinetic and mechanistic information when applied to the study of electrochemical systems [6-11]. Electrochemical impedance spectroscopy (EIS) has been proved to be a very useful technique to investigate corrosion reactions [11-15], and it is widely used for evaluating corrosion protection layers on metallic substrates. The use of EIS has resulted in new information being obtained concerning the painted metal/corrosive electrolyte interface, such as the charges in the corrosion mechanisms and the growth of the reactive area. In fact, corrosion is the result of a number of complex reactions, and many factors are involved. It is difficult to evaluate the contribution of each of these factors, but the electrochemical approach is able to give some helpful information in this respect [1]. One of the advantages of EIS over other techniques is that the measured data can be described analytically employing an equivalent circuit as a model [3]. The elements of an equivalent circuit model represent the microscopic processes involved in the transport of mass and charge.

In this study, DSC and FTIR techniques were used to characterize the curing behaviour of an epoxy/polyester powder coating. In order to evaluate water permeability of the given powder paint and to assist the determination of the corrosion performance of the coated aluminium substrate, an EIS technique was employed.

EXPERIMENTAL

Materials and Methods

1050 Aluminium alloy as 0.5 mm thick sheets in H18 temper were used for all experiments. Polyacrylic acid (PAA), with average molecular weight: 104,000, as a 25% solution in distilled water and fluorozirconic acid (H_2ZrF_6) as a 45 % solution in distilled water, were employed. The samples were treated according to Table 1, before being painted with the following procedure.

A commercial epoxy/polyester hybrid powder coating (supplied by Mega Company, Ral 9016, and with the trade name of White 123 for Interior use) was applied to the pretreated samples using a 405 Stajet electrostatic spray gun. The thickness of the cured powder coated samples was measured using an Elcometer 256 instrument with an accuracy of 0.1 m. Measurements were carried out on a set of five different replicate samples; the powder coating thicknesses varied from 50.2 to 61.4 m.

Differential Scanning Calorimetry (DSC)

DSC Studies were performed by using a 'Polymer Laboratory' Model PL DSC apparatus. DSC Scans were carried in dynamic mode operation. In this way, a few milligram samples of uncured powder were placed in the aluminium DSC pans and their DSC spectra were recorded from room temperature to 250°C at a rate of 10°C/min.

FTIR Spectroscopy

A Perkin Elmer FTIR spectrophotometer, (Spectrum 2000 model) was used. FTIR Spectrum of the as-supplied powder coating was recorded in the form of a disc

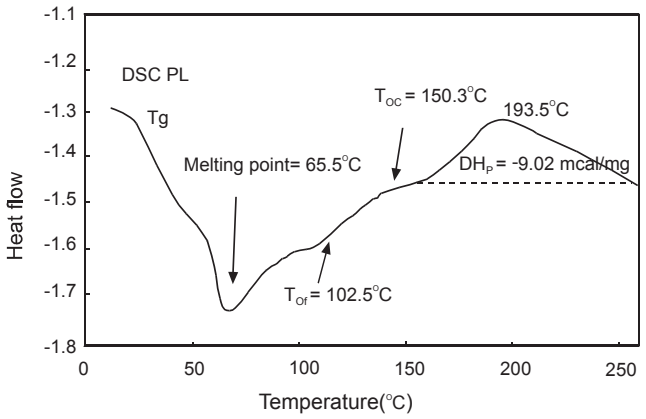

Figure 1. Typical DSC spectrum of an epoxy/polyester powder coating.

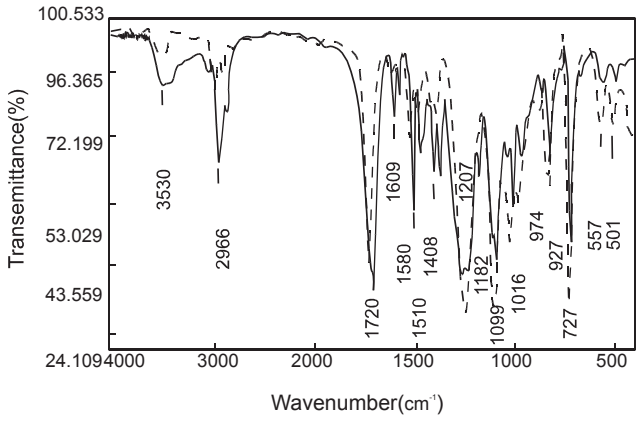

Figure 2. FTIR Spectra of an epoxy powder coating before(-) and after(---) curing.

pressed from 10% by w/w dispersions in dry potassium bromide. Cured powder coating samples were analyzed in a reflection-absorption spectroscopy attachment.

Electrochemical Impedance Spectroscopy (EIS)

EIS Measurements were performed at the open circuit potential using an ACM impedance instrument (AUTO-DSP). The electrochemical tests were carried out in an aerated 3 % NaCl solution. The exposed painted samples had areas of about 36 cm^2. A three-electrode arrangement, with a saturated calomel reference electrode and a platinum counter electrode, was used. The impedance data were obtained as a function of frequency, using a sine wave of 20 mV amplitude; a frequency range from 30 kHz to 10 mHz (10 points per decade) was selected.

RESULT AND DISCUSSION

DSC

A typical non-isothermal DSC spectrum of the epoxy/polyester powder coating is illustrated in Figure 1. From the Figure, two endothermic transitions are evident. The first transition, T_g (uncured powder), occurred at a temperature of about 45°C, while the second, the melting point, showed at a temperature of 65.5°C. As the sample was heated further, the trace started to rise, which indicated that the powder had started to flow, T_{oc}, and this occurred at a temperature of around 102.5°C. On further heating, the trace revealed a small transition indicating that the powder had started to cure, T_{oc} , and this occurred at a temperature of 150.3°C. On still further heating, one principal exotherm was observed corresponding to curing reactions, with a maximum rate of heat evolution at 193.5°C, showing the maximum rate of the curing reactions, which subsequently fell, showing the completion of the heat evolution (curing reactions). It can be deducted from the Figure that the curing reactions of the given powder coating start at approximately 150°C and terminate at about 250°C. The temperature differences between the onset of flow, when the powder starts to flow, T_{oc}, and the onset of cure, when the exothermal reaction begins, T_{oc}, gives an indication of the time available for the powder coating to flow:

$$\frac{(150.3-102.5)°C}{10°C/\min} = 4.78 \text{ min}$$

which can be used in the melt mixing of the extruder.

FTIR

The FTIR absorption of powder coating sample prior to and after curing shown in Figure 2 are assigned [16] in Table 2. FTIR Specrta of the samples before and after curing are very similar, the only difference being in the intensity of the (O-H) absorption band (3503 cm^{-1}). The (O-H) absorption band is less intense for the cured powder sample. The hydroxyl stretching absorption in the cured sample decreased indicating a reduction of hydroxyl content upon curing. The hybrid epoxy systems have fast curing rates, which allow stoving schedules of 10-15 min at 180°C up to 30 min at 140-150°C [17-19]. When the acid /epoxy stochiometry is 1:1, the reaction generates a hydroxyl ester eqn (1), excluding the formation of polyesters, eqn (2).

Table 1. Pretreatments for the 1050 aluminium alloy.

No	Pretreatment	Pretreatment process for aluminium samples
1	Acetone degreased	Hand solvent cleaning in acetone using a soft brush.
2	Etched	(a) Acetone degreasing and (b) 5 min in 5% NaOH solution at 55 ± 5°C, distilled water rinsing and drying in warm air at 45-50°C.
3	De-smutted	(a) Acetone degreasing, (b) etching and (c) 3 min in 50% v/v HNO_3 at ambient temperature, distilled water rinsing and drying in warm air at 45-50°C.
4	CPCC	(a) Acetone degreasing, (b) etching, (c)de-smutting and (d) 5-10 min immersion in 64 g/L H_3PO_4+ 9 g/L Cr_2O_3+3 g/L NaF at 20 ± 1°C; distilled water rinsing and drying in warm air at 50°C.
5	PAA	(a) Acetone degreasing and (b) 30 min immersion in 5,10 and 20 g/L PAA solutions at 20 ± 1°C (dry in place); drying in hot air at 140°C for 30 min.
6	PAA+ H_2ZrF_6 (PZr)	(a) Acetone degreasing, (b) etching, (c)de-smutting and (d) 30 s in 1g/L PAA+1g/L H_2ZrF_6 solution at 20 ± 1°C (dry in place); drying in hot air at 140°C for 30 min.
7	H_2ZrF_6 (Zr)	(a) Acetone degreasing, (b) etching, (c)de-smutting and (d) 30 s in 1 g/L H_2ZrF_6 solution at 20 ± 1°C (dry in place); drying in hot air at 140°C for 30 min.

1- Ring opening of an epoxy group together with reaction with an acid group, leading to formation of a hydroxyl ester.

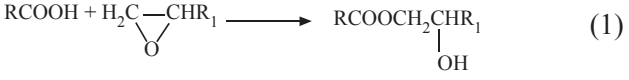

(1)

2- Esterification reaction between an acid group and the hydroxyl group formed in the previous reaction.

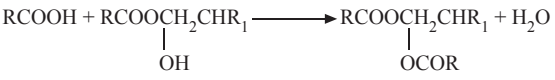

(2)

EIS

Figure 3 shows typical Nyquist plots for differently pretreated powder coated samples, over various immersion times in 3 % NaCl electrolyte. The plots show two semi-circles (except for CPCC treated samples), with two-time constants at frequencies of about 100-200 Hz and 0.5-2.0 Hz, respectively. An equivalent circuit model proposed by many authors [11-15] based on the Nyquist plots for powder-coated samples is shown in Figure 2. This model consists of the electrolyte resistance, R_s, the coating capacitance, C_c, the coating resistance, R_{pf}, the charge transfer resistance, R_{ct}, and the double layer capacitance, C_{dl}. The EIS data were interpreted based on proposed equivalent electrical circuits using a suitable fitting procedure elaborated by Boukamp program software [20]. The results of the analysis and calculations of the impedance data (averaged from five replicate specimens) are given in Figure 5.

Degreased Samples

The coating resistance of the differently pretreated samples during 20 days of immersion in the electrolyte is shown in Table 3. The coating resistance values are varied from 9.3 * 10^8 (0.5 % PAA) to 2.6 * 10^9 (CPCC) ohm.cm^2, which shows that there is little change in the coating resistance and possibly in the uniformity of the films cross-linking. Mayne and Scantlebury [21-22] showed that the solvent-based organic coatings are almost heterogeneous in structure and that this is related to the cross-linking within the film. Variation in the coating resistance may be a result of heterogeneity in the structure [23]. Therefore, it is suggested that the cured powder coatings are more likely to be fully cross-linked. Table 3 also shows that in comparison with the literature [24], the coating resistance is high. It appears that there are no pathways for easy ion transport when the coating resistance is high, whereas the low resistance film had small pathways for easy ion transport. It is considered more likely that the majority of any holes, pores or voids that are probably the basis of conductive

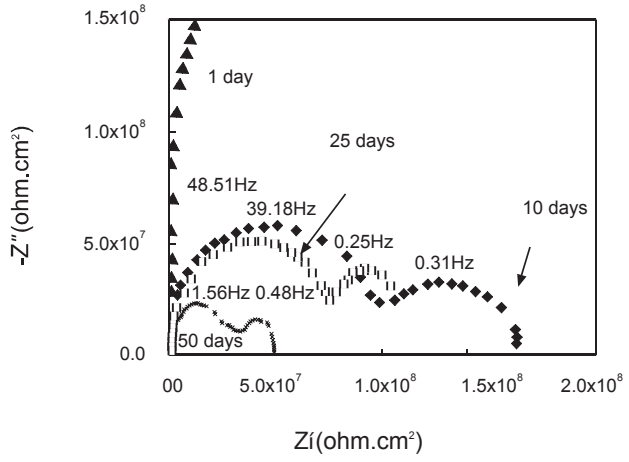

(a) Degreased/powder coated samples.

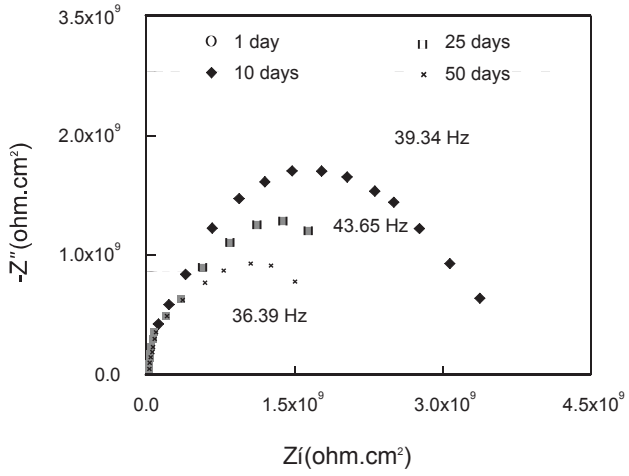

(b) CPCC/powder coated samples.

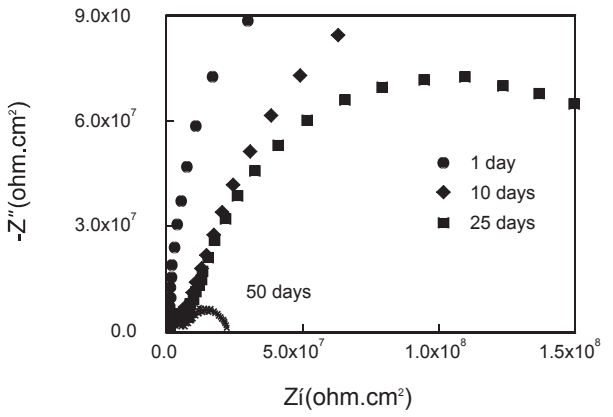

(c) 0.5 %PAA/powder coated samples.

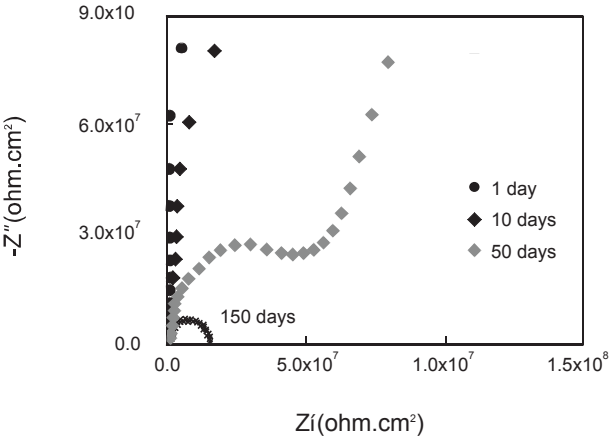

(d) PZr/powder coated samples.

Figure 3. Impedance spectra of powder coated aluminium substrates with immersion time in 3% NaCl electrolyte.

pathway must be the result of incomplete cross-linking of the polymer film.

From Figures 3 and 5, for the degreased substrates, the first measurement (1day) clearly shows capacitive behaviour with a parallel resistive component in excess of 109 ohm.cm^2, probably due to the polymer film [25]. With increasing immersion time (10 days), the radius of the high frequency semi-circle decreased. The coating resistance values (Figure 1a) decrease during first few days of immersion. It is considered that a decrease in the coating resistance value may be due to the penetration of water and movement of ionic species through the coating layer, increasing the coating's conductivity. Initially, the electrolyte penetrates through the coating layer, and sets up conducting paths at different depths within the coating.

Further, a second semi-circle in the impedance spectrum is observed at reduced frequencies, suggesting [6, 26-27] that electrochemical reactions at the interface between the coating and the metal surface are progressing. At this stage, penetration is completed and the electrolyte phase meets the metal/oxide interface and a corrosion cell is activated. With increased immersion time (25 days), the barrier properties of the coating decreased further; however, the radius of the second semi-circle also decreased, suggesting an increase in corrosion rate, possibly through the presence of further pores in the coating or an increase in the area exposed at the base of the existing pores or flaws.

With increasing immersion time, a further increase in the coating resistance was observed; suggesting that pores within the coating layer were blocked [27] with

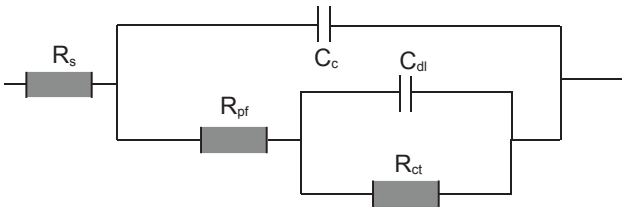

Figure 4. Equivalent circuit for the powder coated aluminium alloy substrates.

corrosion products, and therefore the ionic movement in the coating layer was impeded. With further time, the coating resistance continuously decreased; however, the radius of the second semi-circle also decreased, again suggesting an increase in the corrosion rate possibly through the generation of further pores in the coating or an increase in the exposed area of the existing pores or flaws.

The values of the coating capacitance increase during the initial period of immersion due to uptake of water; subsequently the capacitance remains almost constant (saturation of the coating layer with water) and after 20 days it increases further it. As partial explanation this may arise from water accumulation beneath the coating.

The value of C_{dl}, which is related to the area of the substrate in contact with the electrolyte because of loss of adhesion, increases with immersion time, while the R_{ct} values, which are inversely proportional to the corrosion rate, decrease.

A high value of R_{ct} (Figure 3c) for the degreased sample indicates that the corrosion rate is relatively low, during the first 20 days of immersion time. After 20 days, the charge transfer resistance decreased dramatically, suggesting an increase in the corrosion rate, possibly through the presence of new pores in the coating or an increase in the area of the existing pores or flaws. After 30 days, R_{ct} increased. This is possibly due to pore blocking with corrosion products. After 75 days, the value of the R_{ct} decreased. The decrease of charge transfer resistance and increase in double layer capacitance indicate an increase in corroded area under the coating as a consequence of progressive degradation.

CPCC Treated Samples

For the CPCC coated substrates (Figure 3b), the spectra reveal capacitive behaviour and a resistive component greater than $2 * 10^9$ ohm.cm^2. The coating resistance decreased to some extent with increasing exposure time, and reached a constant value after 25 days. No damage or delamination was observed. It is evident that the impedance values recorded for CPCC treated samples are higher than impedance values obtained for degreased samples, indicating the beneficial role of chromium species affecting the overall coating resistance.

Table 2. FTIR Assignments of an epoxy powder coating prior to and after curing [16].

Uncured powder	Cured powder	Assignment
3503 b	3495 b	ν(O-H), hydrolyzed epoxide
2966 s st	3020 m	ν(O-H), OH (acid)
3000-2850 m	3000-2850 m	ν(C-H), CH (aliphatic)
1720 s st	1722 s st	ν(C=O), on epoxide ring
1725-1700 s st	1725-1700s st	ν(C=O), COO (acid)
1570 s m	1570 m	$\nu_a(COO^-)$, acid salt
1550 m	1550 m	COO^-, H^+, ionized form
1450 s m	1448 s m	$\delta(CH_2)$, CH_2
1408 s st	1416 s m	δHC(CO), CH-CO
1300-1200 s st	1300-1200s st	CO-O-R, C-O,
1099 s st	1100 s st	ν(C-O), aromatic (C-H)
1016 s m	1012 s w	ν(C-O)
727 s st	727 s st	$\delta(CH_2)$, $-CH_2-$

b: broad, s: sharp, st: strong, m: medium, w: weak

CPCC contains insoluble hydrated chromium phosphate [28], which may act as an efficient barrier to corrosion [29]. Cr(VI) may be included in the conversion coating and is reduced at flaws [30] to Cr(III) to re-passivate any damaged surface. In the absence of pretreatment, the substrate is active and the resistance is low when corrosion occurs. In the absence of a passive layer (CPCC) and the presence of under-film corrosion, the coating resistance is low because of the processes of ionic current flow on the surface due to the presence of anodic and cathodic sites, ionic migration within the film (electrolyte), localized film changes and electro-osmotic movement of water [31]. Flaws, always present in air-formed films, are important in localized corrosion, and pitting [32]. The cathodic reactions proceed at impurity segregates at residual flaws. The cathodic

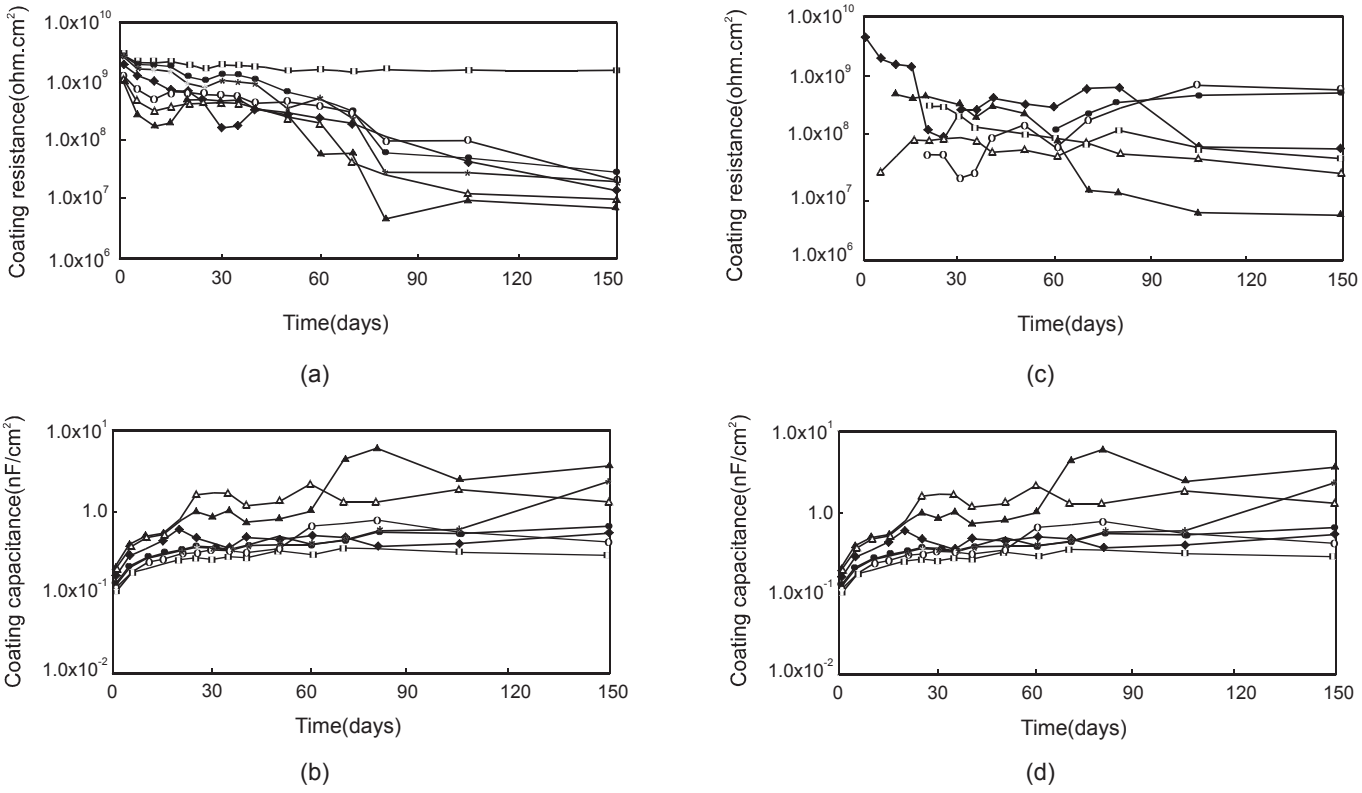

Figure 5. (a) Time dependence of coating resistance;(b) Time dependence of coating capacitance; (c) Time dependence of charge transfer resistance and (d) Time dependence of double layer capacitance for powder coated Al samples with different pretreatments during 150 days immersion in 3% NaCl solution.(—◆— Deg; —△—5PAA; —○—10PAA ; —▲— 20 PAA ; —□—CPCC; —●— Pzr; —*— Zr.

reaction is either reduction of oxygen or hydrogen generation.

PAA Treated Samples

Figure 3c indicates the relatively poor barrier properties of PAA treated samples. This is due to the hydration of aluminium oxide at the water-rich interface [33], with the water being replaced by aluminium hydroxide and PAA-oxide bonds.

It has been suggested [34] that hydrated aluminium oxide decreases the stability of adhesive joints in presence of water. The coating layer may detach from the metal substrates at the metal/coating interface due to diffusion of both water and oxygen through the coating. Water penetrates through the coating with time, and reaches the coating/metal interface. Water may solvate PAA molecules, resulting in a loss of adhesion. The high hydroxyl ion concentration dissolves the aluminium oxide and the aluminium metal possibly attacks the PAA molecules at the interface between the polymer and the substrate.

PZr Treated Samples

From Figure 3d, for PZr treated samples, the spectra are dominated by the capacitance of the coating, which remained constant (other than for one sample) after more than 50 days exposure to 3 % NaCl electrolyte. It is clear that the impedance values recorded for PZr treated samples are higher than the impedance values obtained for degreased and PAA treated samples. Zr and PZr pretreated samples reveal relatively good corrosion performance over the first 50 days of immersion in the electrolyte.

It is proposed [35] that zirconium-based treatments may protect the surface against the corrosive environment, by the reduction of anodic reactions over the aluminium surfaces; consequently the passivity of the metal increases. The action of zirconium-based pretreatments and generation of pseudoboehmite films in boiling water treatments, are considered to be similar

Table 3. The coating resistance (Ohm.cm^2) of the differently pretreated powder-coated samples during 20 days of immersion in 3 % NaCl electrolyte.

Pretreatment	Immersion time		
	1 Day	5 Days	20 Days
Deg	$1.6 * 10^9$	$1.2 * 10^9$	$6.3 * 10^8$
CPCC	$2.6 * 10^9$	$1.9 * 10^9$	$1.7 * 10^9$
0.5 % PAA	$9.3 * 10^8$	$4.2 * 10^8$	$2.9 * 10^8$
1.0 % PAA	$1.1 * 10^9$	$6.8 * 10^8$	$5.9 * 10^8$
2.0 % PAA	$1.0 * 10^9$	$2.7 * 10^8$	$4.6 * 10^8$
PZr	$2.5 * 10^9$	$1.8 * 10^9$	$1.1 * 10^9$
Zr	$2.2 * 10^9$	$1.5 * 10^9$	$8.7 * 10^8$

[35-38].

A further possibility is that when a polymer is present in the conversion coating solution (e.g., for the zirconium-based pretreatments), it may act as a surfactant and modify the conversion coating. It is suggested [39] that PAA molecules assist in the production of a uniform conversion-coating layer on the surface.

CONCLUSION

- The powder coating curing process starts at approximately 150°C and terminates at about 250°C with a heating rate of 10°C/min.

- EIS May be used for characterizing the corrosion protection properties of coated metallic substrate. In this way, the durability of the coatings can be predicted before changes in the appearance of the coating are visible to the eye.

- EIS is a valuable test method for predicting the durability of coatings.

- Relatively good performance of the powder coating is due to a high ohmic resistance of the coating prior to and after saturation with water and the reasonably low water solubility of the powder coating.

- The degreased samples showed a better performance than PAA treated samples. However, CPCC treated specimens showed no visible change after completion of the test. PZr and Zr treated samples revealed good performance over 60 days of immersion time. Subsequently, their performance decreased, with the samples behaving similarly to the degreased samples.

REFERENCES

1. Howell D.M., Powder Coatings: *The Technology, Formulation and Application of Powder Coatings,* Sanders J.D., Ed., **1**, John Wiley, London UK (2000).
2. Belder E.G., Rutten H.J.J., and Perera D.Y., Cure characterization of powder coatings, *Prog. Org. Coat.,* **42**, 142-149 (2001).
3. Hess J., Powder coatings everywhere, *Coating World*, **36**, 33-37 (1999).
4. Leidheiser H. Jr., Corrosion of painted metals - A review, *Corrosion-NACE,* **38**, 374-383 (1982).
5. Mayne J.E.O., Anti corrosion method and materials, **10**, 3-7 (1973).
6. Deflorian F., Fedrizzi L., Lenti D., and Bonora P.L., On the corrosion protection of fluoropolymer coatings, *Prog. Org. Coat.,* **22**, 39-53 (1993).
7. Silverman D.C., *Electrochemical Techniques for Corrosion Engineering,* Boboin R., Ed., NACE, 73-79 (1986).
8. Van Westing E.P.M., Ferrari G. M., and De Wit H.W., The determination of coating performance with impedance measurements - III. In situ determination of loss of adhesion, *Corrosion Science,* **36**, 979-994, (1994).
9. Mansfeld F., Recording and analysis of AC impedance data for corrosion studies, *Corrosion-NACE,* **36**, 301-307 (1981).
10. Deflorian F., Fedrizzi L., and Bonora P.L., Impedance study of the corrosion protection of flouropolymer coatings, *Prog. Org. Coat.,* **23**, 73-88 (1993).
11. Pistorius P.C., Electrochemical testing of 'Intact' organic coatings, *4th Int. Corro. Cong.,* Cape Town, 26 Sept. (1999).
12. Sastri S.V., *Corrosion Inhibitors,* John Wiley, New York (1998).
13. Sykes J.M., 25 Years of progress in electrochemical methods, *Br. Corrosion,* **25**, 175-183 (1993).
14. Walter G.W., A review of impedance plot methods used for corrosion performance analysis of painted metals, *Corrosion Sci.,* **6**, 681-685 (1986).
15. Mansfeld F., Kendig M.W., and Tsai S., Evaluation of corrosion behavior of coated metals with AC impedance measurements, *Corrosion NACE*, **38**, 478-482 (1982).
16. Grapper G.D., Synthesis and properties of epoxy/polyester-based powder coatings, Ph.D. Thesis, Manchester University, Material Science Centre (1993).
17. Misev T.A., *Powder Coating, Chemistry & Technology,*

John Wiley, New York (1991).
18. Yaseen M. and Funke W., Effect of temperature on water absorption and permeation properties of coatings, *JOCCA,* **61**, 284-291 (1978).
19. Bate D.A., *The Science of Powder Coatings,* **1**, SITA Technology (1990).
20. Boukamp B.A., *Equivalent Circuit, A Package for Impedance/Admittance Data Analysis,* University of Twente, **89** (1986).
21. Mayne J.E.O. and Scantlebury J.D., Ionic conduction in polymer films, Part II, *Br. Polym. J.,* **2**, 240-243 (1970).
22. Mayne J.E.O. and Scantlebury J.D., Ionic conduction in polymer films, Part IV, *Br. Polym. J.,* **3**, 237-239 (1971).
23. Mayne J.E.O. and Mills D.J., Structural changes in polymer films. Part 1: The influence of the transition temperature on the electrolytic resistance and water uptake, *J. Oil & Col. Chem. Assoc.* (JOCCA), **65**, 138-142 (1982).
24. Kinsella E. and Mayne J.E.O., Ionic conduction in polymer films, Part I, *Br. Polym. J.,* **1**, 173-176 (1969).
25. Mc-Queen R.C., Miron R.R., and Granata R.D., Method for corrosion inhibitor mechanism studies in epoxy coated aluminium, *Coatings Tech. J.,* **68**, 75-82 (1996).
26. Kendig M., Mansfeld F., and Tsai, Determination of the long term corrosion behavior of coated steel with A.C. impedance measurements, *Corrosion Sci.,* **23**, 317-322 (1983).
27. Hepburn B.J., Callow L.M., and Scantlebury J.D., Electrochemical impedance of coated metal electrodes. Part 6: The effect of acid media, *J. Oil & Colour Chem* Association, **7**, 193-196 (1984).
28. Mirabedini S. M., Ph.D. Thesis, The Role of the Interfacial Layer on the Performance of Powder Coated Aluminium Alloy, Corrosion & Protection Centre, UMIST (2000).
29. Treacy G.M., Wilcox G.D., and Richardson M.O.W., Monitoring the corrosion behaviour of chromate-passivated aluminium alloy 2014 A-T6 by electrochemical impedance spectroscopy during Salt Fog exposure, *Surf. Coat. Tech.,* **114**, 260-266 (1999).
30. Thompson G.E. and Wood G.C., *Treatise on Materials Science and Technology* Scully J.C., Ed., Academic, New York, 23 (1983).
31. Crossland A.C., Habazaki H., Shimizu K., Skeldon P., Thompson G.E., Wood G.C., Zhou, and Smith G.J.E., Residual flaws due to formation of oxygen bubbles in anodic alumina, *Corrosion Sci.,* **41**, 1945-1954 (1999).
32. Richardson J.A. and Wood G.C., A study of the pitting corrosion of Al by scanning electron microscopy, *Corrosion Sci.,* **10**, 313-323 (1970).
33. Mirabedini S.M., Moradian S., Scantlebury D.J., and Thompson G.E., Polyacrylic acid as a surface pretreatment for 1050 aluminium alloy, *2nd Inter. Symp. Alum. Surf. and Sci. Technol.,* 21st-25th May, UMIST, UK, 485-490 (2000).
34. Dickie R.A., Paint adhesion, corrosion protection, and interfacial chemistry, *Prog. Org. Coat.,* **25**, 3-22, (1994).
35. Deck, P.D., Moon, M., and Sujdak, R.J., Investigation of fluoroacid based pretreatments on aluminium, *Surface Coat. Inter.,* **10**, 478-485 (1998).
36. Das N., *US Patent,* 3964936, Coating solution for metal surfaces, (1976).
37. Nelson J. and Newhard Jr., *Corrosion Control by Coatings,* H. Leidheiser, Ed., 225-241 (1978).
38. Lytle F.W., Greegor R.B., Bibins G.L., Blohowiak K.Y., Smith R.H., and Tuss. G.D., An investigation of the structure and chemistry of a chromium conversion surface layer on aluminium, *Corrosion Sci.,* **37**, 349-369, (1995).
39. Hatanaka K., Fukui M., and Mukai Y., Coating adhesion of polyacrylic acid-zirconium composite treated aluminium, *Kobelco Tech. Rev.,* **10**, March (1991).